Seasonal Influence on Aluminium Cell Heat Balance and Performance

Eirik Manger[1], Asbjørn Solheim[2] and Nancy Jorunn Holt[3]
1. Principal Engineer, Technology and Operational Support, Hydro Aluminium, Norway
2. Chief Scientist, SINTEF Industry, Norway
3. Program Manager, Technology and Operational Support, Hydro Aluminium, Norway
Corresponding author: eirik.manger@hydro.com

Abstract

Some aluminium smelters in Norway occasionally experience hot cell sides and reduced current efficiency during the summer season. The increase in cell side temperatures is typically larger than what would be expected from modelling, where such changes are usually said to roughly follow the ambient temperature. The root cause of this phenomenon is not fully known, even though being subject to substantial research for years. In this paper we discuss different mechanisms that could contribute to such a behaviour. These contributions are theoretically evaluated and analysed in combination with results from targeted experiments and measurement campaigns. Furthermore, a detailed pot room model has been established looking at the effects of ventilation – cooling due to ventilation is probably the most difficult to measure and (perhaps) the easiest to model. The simulations confirm that the pot shell, if seen as isolated with no heat flux change, indeed follows the ambient temperature increase with some dependence on the initial conditions. Our results show that several different mechanisms contribute to higher cell side heat fluxes during summers, some more than others. However, the results also indicate that these mechanisms alone may not explain the observed operational behaviour. A new hypothesis is presented, suggesting that decreased current efficiency as the Anode-Cathode Distance (ACD) is squeezed might be another source for the temperature increase seen.

Keywords: Aluminium electrolysis cells, Cell performance, Hot cells, Pot room ventilation, Anode cathode distance.

1. Introduction

Aluminium electrolysis cells are dependent on having a protective layer of frozen electrolyte on the inner walls. The delicate energy balance entails that the cell can function only within a certain (narrow) range of operating parameters mainly defined by the cathode design. This implicitly limits the current, since a larger quantity than acceptable would generate too much heat. Still, it has been possible to improve the performance considerably for given cell technologies (capacity creep). As an example, the productivity in four Hydro Aluminium plants was increased by nearly 40 % from 1983 to 2006, while at the same time reducing the specific energy consumption [1]. Enabling factors included longer anodes, increased anode stub diameter, new cathode designs, new side-lining materials, and lower anode-cathode distance (ACD). All these enhancements have been utilized fully in the new HAL4e technology at the Karmøy Technology Pilot (KTP) [2, 3]. However, there are restrictions to every improvement, and the technology may be pushed to the limit in some locations.

In some plants it was observed that cell performance deteriorates during the summer months ("summer effect"). The pot shell temperature increases, sometimes much more than the ambient temperature, and the current efficiency (CE) decreases. Modelling tools struggle to reproduce these seasonal variations. The effect of ambient temperature on aluminium electrolysis cells' performance is also scarcely treated in the open literature, although exceptions can be found [4]. It was decided to carry out a theoretical and experimental study to reveal the root causes for the variations. The purpose of the present paper is to present some hypotheses on what is causing the

"summer effect". Estimates, calculations, modelling results, and experimental data are presented, aiming to reveal the relative importance of different effects. The study is still ongoing. Although the results are not conclusive, it appears that there must be several reasons for the "summer effect".

2. The Challenges

There is no doubt that the last decades' systematic performance improvements, increased data acquisition and better accuracy have given both opportunities and challenges. As shown in the introduction, technologies are pushed and squeezed to increase nominal production, and the cells operate with tighter margins and less tolerances for deviations. However, enhancements tend to follow cell generation changes, and explanations that at some point seem rather obvious might take several years to reveal.

Relations between ambient conditions and pot shell temperatures have been subject in a previous study. Haugland et al. [4] reported measurements showing correspondent ambient and pot shell temperature changes, which fit quite well with Computational Fluid Dynamics (CFD) calculations presented below. However, in the recent years some smelters have seen deviations from this 1:1 correspondence. Recent long-term measurements have shown significantly larger pot shell temperature changes compared against ambient temperature, see Figure 1. The seasonal variations do follow each other, but the absolute values have ratios close to 2.5:1. Maximum "average" ambient differences somewhat above 30 °C have given rise to around 80 °C shell temperature variation. Higher pot shell temperatures are undesirable, as these give lower margins for errors and cause disturbances and challenges for the operations.

In addition to hot pot shells, smelters also report decreased CE during the summer season. No absolute figures will be given, and the reader will acknowledge that CE with such quite small time periods as 3-4 months could be contaminated with relatively large errors. Still, the trend is clear, with a seasonal variation also in CE. Presumably these changes are connected.

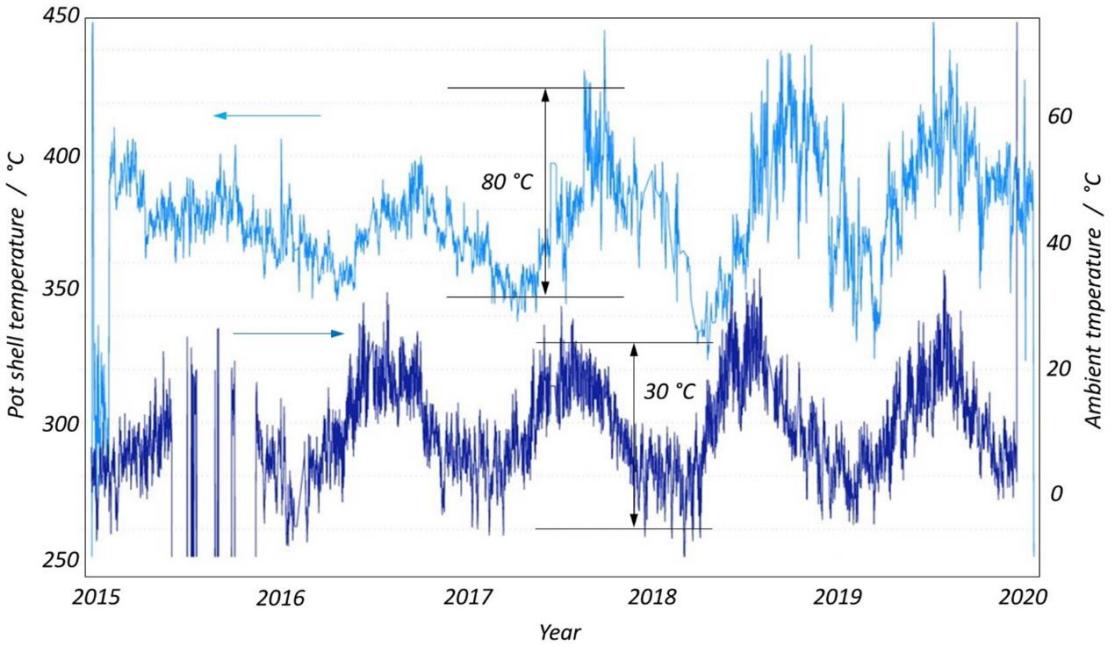

Figure 1. Example of pot shell and ambient seasonal temperature variations. Note the difference between the y-axes, which have ratio 2.5:1.

3. Initial Hypotheses and Theoretical Considerations

A broad investigation path was followed in the start of this study, having a primary goal to find and understand all possible effects that could contribute to hot pot shells with higher ambient temperatures. Several mechanisms were identified, where three hypotheses were selected for further evaluation.

Hypothesis 1: The convective heat transfer coefficient at the pot shell will decrease with increasing temperature. On the other side, thermal radiation becomes more efficient. Either way, higher ambient temperature gives higher pot shell temperatures, and thereby initially lower heat flow through the sides. The cell becomes hotter, which will be compensated by melting away ledge. It is known that a thinner side-ledge gives lower CE [5, 6].

Hypothesis 2: The fans sucking air and process gas through the scrubber normally operate at the same rotational speed during all seasons. This means that the volumetric flow out of the cells is nearly constant, in a seasonal perspective, whereas the mass (or molar) flow decreases when the temperature increases. As a result, the temperature in the off-gas increases not only due to the increased ambient temperature, but also because the mass flow (Nm^3/h) decreases. This gives lower heat loss upwards, and more heat must be evacuated through the cathode sides.

Hypothesis 3: Increasing ambient temperature gives higher temperature in the external current circuit (busbars, collector bars outside the pot shell, risers, and anode beam). As a result, the external resistance increases. Keeping the controller set point unchanged requires a reduced ACD since the controller does not distinguish between external and internal resistance. Not reaching the set point would lead to increased total resistance and more heat generation. On the other side, a reduced ACD may induce lower CE.

3.1 Temperature Variation of Heat Transfer Coefficients

The convective heat transfer coefficient depends on viscosity, thermal conductivity, and the coefficient of thermal expansion – all functions of temperature. The coefficient can be estimated from correlations such as suggested by Churchill et al. [7]. The radiative heat transfer coefficient can be defined as the heat flux calculated from the Stefan-Boltzmann law divided by the temperature difference. The convective and the radiative heat transfer coefficients are additive.

To illustrate the temperature dependence, the convective heat transfer coefficient was calculated from standard dimensionless equations with data for air [8, 9]. The wall temperature was assumed to be 300 K above ambient temperature. Physical data for air was evaluated at the film temperature (arithmetic average of the wall and ambient temperatures). The relative values of the heat transfer coefficient are shown in Figure 2.

The convective heat transfer coefficient decreases with increasing temperature, both if assuming forced turbulent convection or natural convection, while the radiative heat transfer coefficient increases. However, the variation of the total heat transfer coefficient does depend somewhat on local conditions at the pot shell, such as geometry (view factors) and air flow. Thus, the relative magnitude between these mechanisms could vary. Still, it is fair to assume that the total heat transfer coefficient does not vary much with the ambient temperature, which implies that the temperature difference between the pot shell and the ambient air is close to constant at constant heat flux.

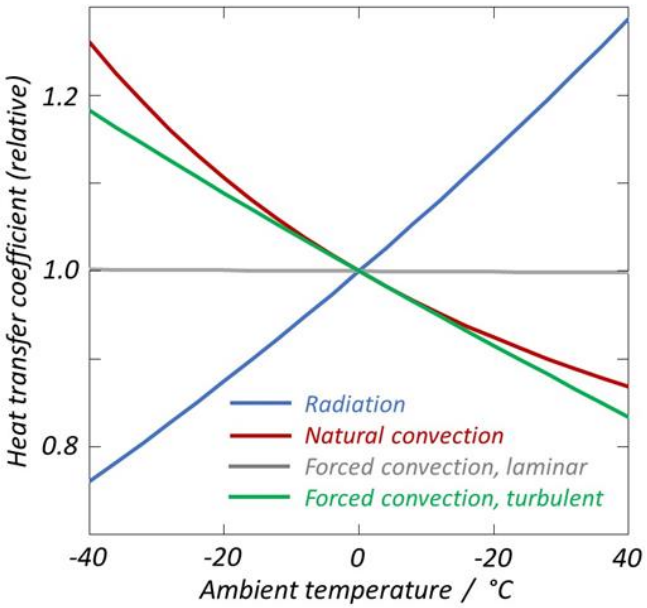

Figure 2. Heat transfer coefficients as a function of the ambient temperature (relative values, 0 °C = 1). The wall temperature is assumed 300 K above the ambient temperature and the physical data were evaluated at the film temperature.

3.2 Mass Flow Variations through the Off-gas System

Since the flow through the off-gas system normally is controlled either by volume or fan workload (i.e., pressure drop), the mass flow and equivalently the heat evacuation will vary with ambient temperature. Assuming that the volume flow is constant, there is a linear relationship with temperature, expressed as in Equation (1).

$$\Delta \dot{m} = \dot{m}^1 - \dot{m}^0 = \left(\frac{T^0}{T^1} - 1 \right) \cdot \dot{m}^0 \tag{1}$$

where $\dot{m}$ is the mass flow rate, T is temperature, and superscripts 0 and 1 refer to before and after a change. If keeping constant load on the fans and disregarding the fan operation curve, the pressure drop is approximately proportional to the dynamic pressure, $\Delta p \sim \rho v^2$. An upper limit for volume flow increase with temperature is then given from

$$\Delta \dot{V} = \dot{V}^1 - \dot{V}^0 = \left(\sqrt{\frac{T^1}{T^0}} - 1 \right) \cdot \dot{V}^0 \tag{2}$$

where $\dot{V}$ refers to the volume flow rate, and the corresponding mass flow change becomes

$$\Delta \dot{m} = \dot{m}^1 - \dot{m}^0 = \left(\sqrt{\frac{T^0}{T^1}} - 1 \right) \cdot \dot{m}^0 \tag{3}$$

The true picture will be somewhere between correlations (1) and (3), since fan power is proportional to pressure drop as well as volume flow. Both correlations have been used to plot the relative change in mass flow through the off-gas system, alternatively increased off-gas

temperature if maintaining the mass flow, as shown in Figure 3. Original off-gas temperature was assumed 100°C above ambient.

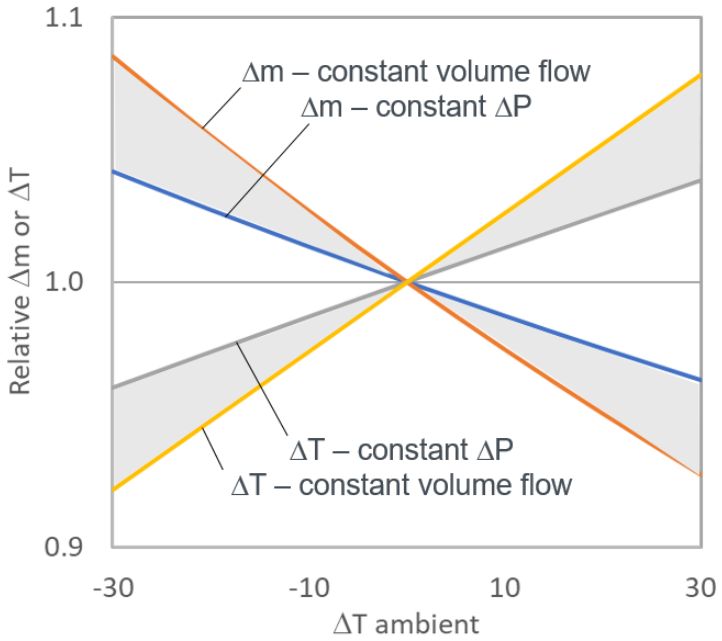

Figure 3. Mass flux (proportional to energy removal) and temperature change through the off-gas system as a function of the ambient temperature (relative values, 0°C = 1). The shaded areas represent the possible range of relative values.

3.3 Increased Electrical Resistance through the External Current Circuit

3.3.1 External Resistance and ACD

It is a fact that electrical resistance in metals increases with temperature. Within small relative changes, the variation can be estimated according to a linear relationship, i.e.

$$\Delta U_{ext} = U_{ref} \cdot (1 + \alpha \cdot \Delta T) \tag{4}$$

where U_{ext} is the voltage drop in the external circuit and anode assembly metal parts, U_{ref} is the voltage drop at the reference temperature and α is the temperature coefficient. Various metals respond differently, typical values are 0.004 K^{-1} for aluminium and 0.006 K^{-1} for steel. Provided that the amperage and total cell voltage are kept constant, an increase in external voltage gives a corresponding decrease in the ACD and bath voltage according to

$$\Delta\delta = -\frac{\Delta U_{ext} \cdot \kappa}{i} \tag{5}$$

where δ is the ACD, κ is the electrical conductivity of the bath (~215 $\Omega^{-1}m^{-1}$) and i is the current density (9500 A/m^2). By taking the reference temperature voltage drop to be 0.2 V for the aluminium parts and 0.24 V for the steel parts and the bimetal plate in the anode assembly, a temperature increase of 40 °C gives a reduction in ACD of 2.0 mm.

3.3.2 ACD and Current Efficiency

It is known that decreasing ACD gives reduced CE in aluminium electrolysis cells when the ACD is below a certain lower limit [10]. It has been suggested that the reason might be that the largest gas bubbles at the anode and the highest waves in the metal start to collide below a certain ACD limit [11]. The latter hypothesis was elaborated in a recent work [12], where the loss in CE was modelled as the result of overlapping Gaussian distribution curves for metal waves and gas bubbles. The results are shown in Figure 4.

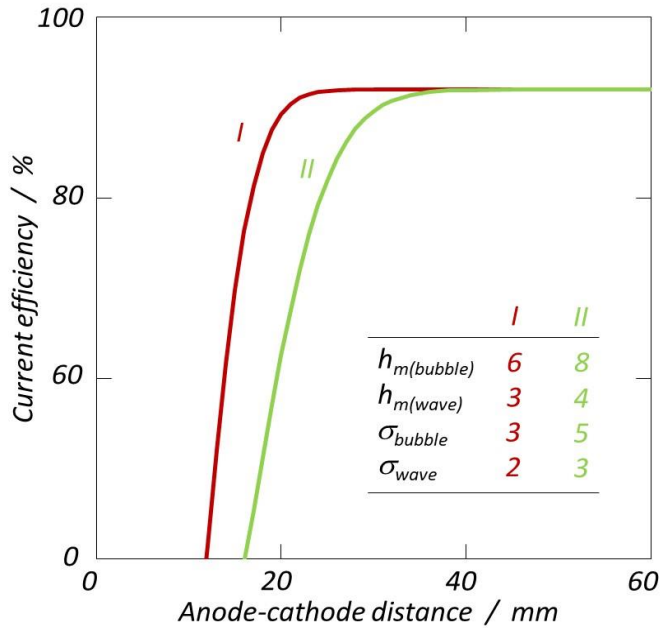

Figure 4. CE as a function of the ACD. The CE was taken to be 92 % when there is negligible overlap between bubbles and metal waves. The average height (h_m, mm) and the standard deviation (σ, mm) for waves and bubbles are given on the graph. Case I and Case II may be taken to represent a slotted anode and a non-slotted anode, respectively (Figure taken from Solheim [12]).

The question is if 1-2 mm reduction in ACD is sufficient to bring about a substantial decrease in the CE, if the cell is already at the critical ACD limit. Low CE means that less electric energy is consumed in the cell reaction, which gives more heat to get rid of. At a certain point, this effect may dominate over reduced Joule heating due to reduced ACD. The curves in Figure 4 were approximated by the function

$$For\ ACD < ACD_{crit}: \quad CE = CE_{crit} + 0.8 \cdot \left\{1 - \exp\left[\left(ACD_{crit} - ACD\right)^{0.6}\right]\right\} \tag{6}$$

The Joule heating in the anode-cathode region was readily determined, and the enthalpy for the total cell reaction including loss in CE was computed from data found in NIST-JANAF [13]. Figure 5 indicates that the reduced energy consumption in the cell reaction starts dominating when the ACD is about 4 mm lower than the critical ACD.

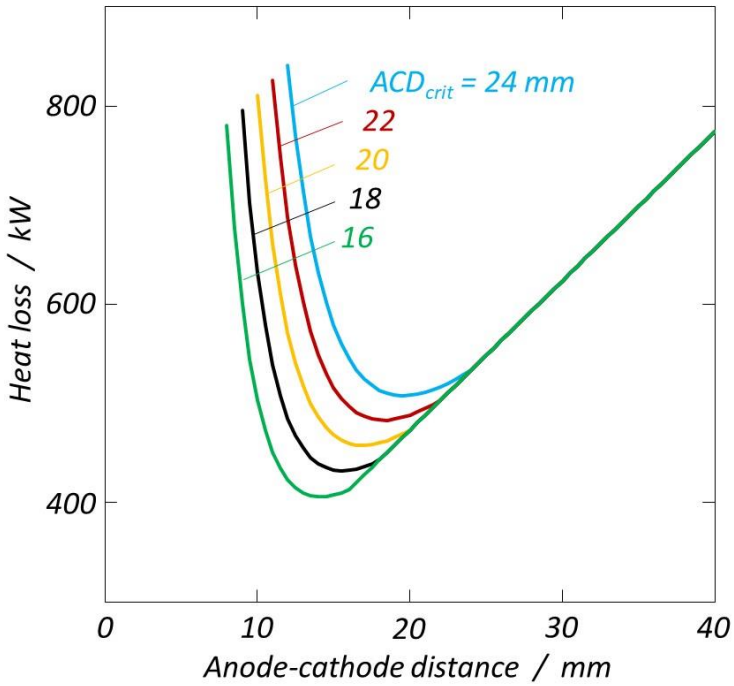

Figure 5. Heat loss as a function of the anode-cathode distance with different values for the critical ACD. See the text for assumptions.

3.3.3 Magnetohydrodynamic Instability

The hypothesis concerning collisions between metal waves and gas bubbles outlined above was developed with only gas induced metal waves in mind. However, magnetohydrodynamic (MHD) instability may play a role, since the resulting slow rotating wave can bring the metal close enough to the anode to entail metal-gas contact in periods, even when the average ACD is far from the critical ACD for gas-metal contact. This is illustrated in Figure 6. As can be observed, a part of the cell may have excessive loss in CE due to contact between bubbles and gas induced waves when the amplitude of the MHD instability wave entails that the local ACD is lower than the critical ACD.

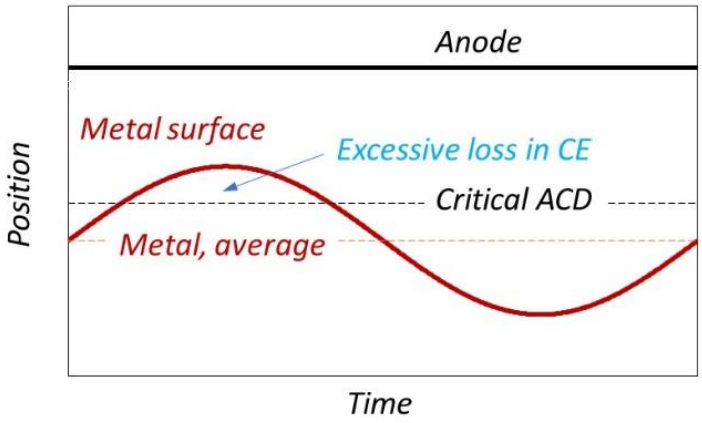

Figure 6. Position of the anode, the metal surface, the average metal level, and the critical ACD for contact between bubbles and gas induced metal waves. The time scale covers one period of the MHD wave.

The local CE for $ACD < ACD_{crit}$ was computed, as shown in Figure 7. The average CE is the time-averaged value for calculations like those shown in Figure 7. The important factors will be the factor $f = ACD - ACD_{crit}$ and the amplitude of the MHD instability wave.

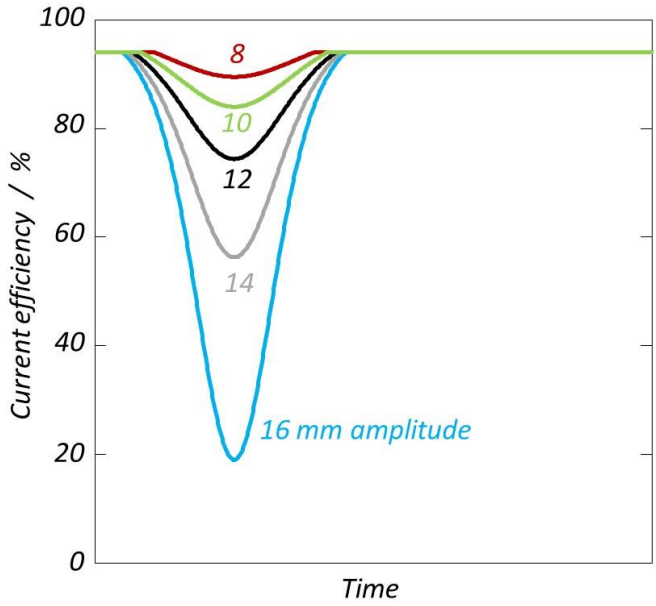

Figure 7. Local current efficiency as a function of time, calculated from Equation 6 with CE_{crit} = 94 %, average ACD = 28 mm, and critical ACD for metal-wave contact ACD_{crit} = 23 mm. The numbers in the graph represent the amplitude of the MHD instability wave. The time scale covers one period of the MHD wave. See also Figure 6.

4. Modelling and Measurements

The purpose, but also the difficulty with performing measurement, are to single out the individual mechanisms as they are all interlinked. On top of this, the ventilation properties are never stable, constantly changing with wind speed, direction, and ambient temperature. Thus, the effect of ventilation was modelled, whereas there were tailored experiments to inspect contributions from forced pot shell cooling and reduced off gas suction.

4.1 A CFD Model to Investigate Shell Cooling

Ventilation modelling of pot rooms is a part of the standard analyses in Hydro, normally done in all new and modification projects. For such calculations, the thermal boundary conditions are given as heat fluxes, and the cell surface temperatures are in general of less interest. However, tailoring the CFD models towards detailed simulations of the pot shell cooling does put stricter requirements on the mesh, particularly near wall surfaces. Since differentiating between convective and radiative heat transfer is a major purpose in such calculations, the boundary layers must be properly resolved to yield good results. See Figure 8 for some geometric details and a segment of the mesh used in the simulations.

A range of simulations were performed with the established CFD model. Mesh sensitivity tests were done, and effects of surface emissivity coefficients were investigated. The numbers presented in Figure 9 are as accurate and representative as possible, given variations in both ambient temperature and heat flux. The results show that average pot shell temperature increases

are marginally higher than ambient changes if keeping all other factors constant. Moreover, the calculations show that the areas with highest initial temperatures have smallest increases, whereas the increase is largest where the starting temperature was lowest. This is reasonable since radiative heat transfer will dominate at higher temperatures.

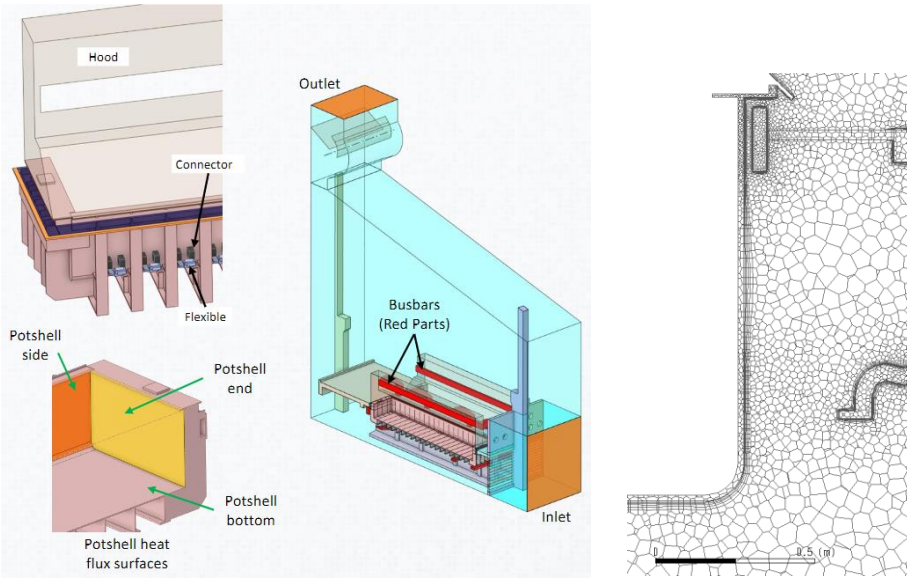

Figure 8. Geometry used for studying cell cooling due to ventilation (left), and part of the mesh showing resolution close the cell side and around flexibles (right).

The calculations also show that a 2.5 % heat flux increase only adds some 4-5 °C to the pot shell temperature. This indicates that the "summer effect", showing temperature differences as large as 70-80 °C, do impose a significantly higher heat flux through the cell sides than 2-3 % – there has to some other contributing effects. Finally, although not included specifically here, simulations have shown that moderate changes of ventilation rates only alter the cell temperatures marginally.

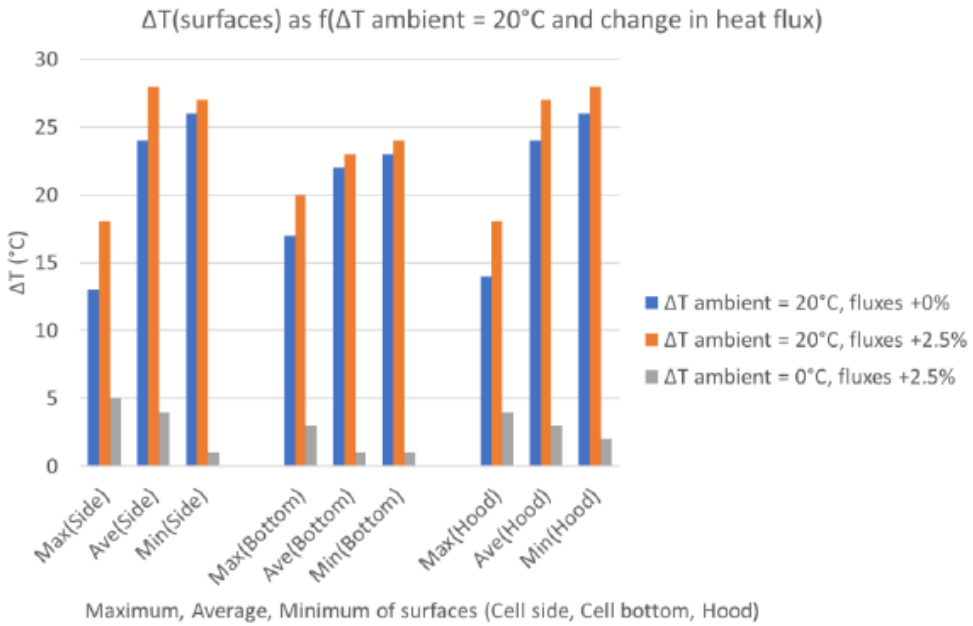

Figure 9. Summary of cell temperature changes, subject to increase in ambient temperature and/or somewhat increased heat flux.

4.2 Experiments with Forced Cooling

Aiming to really see the effects of ventilation rates, we conducted experiments with forced cooling on some pots at a smelter during the last three summer seasons. The additional flow is only a small mass flux to provide some motion in-between the cradles and around the flexibles, see Figure 10 for some pictures on the setup used. Note that the fans supplying air were not installed at the time of the photo.

The number of supply pipes between the cradles were configured so that approximately every second slot received additional air. The cooling equipment was installed on selected pots in the beginning of June, and the cooling effect was monitored by tracking shell temperature at selected positions. The energy consumption and sodium (Na) levels were extracted during the entire test period and compared to results obtained before the cooling started.

Figure 10. The test setup that was used to cool between the cradles and around the flexibles.

Temperatures of the order 380°C were measured around the C-point during the campaign (C-point: metal-bath interphase). When adding cooling air, these were typically lowered with more than 100°C, even though the air flow is considered quite moderate and in addition ejected a good distance away from the monitoring points. The reduced temperature will give more side ledge in the test pots compared against the reference pots.

Both energy consumption and sodium values indicate that the test cells had better performance that the rest of the cells during summer, see Figure 11. The results show that the energy consumption for the test cells increased with 0.41 kwh/kg Al during the cooling period while similar figure for the entire smelter was 0.55 kwh/kg Al. The corresponding sodium level was reduced with 7.5 ppm for the test pots and 9.7 ppm for some reference pots.

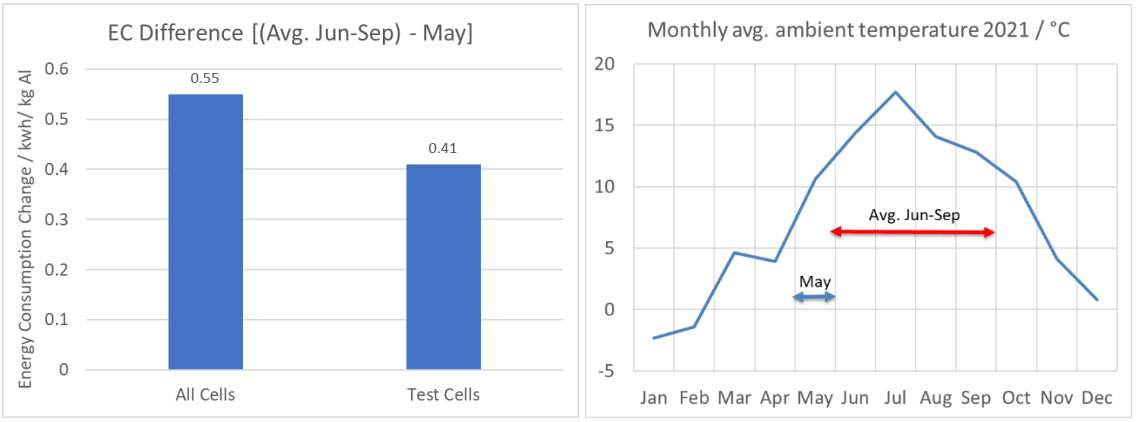

Figure 11. Energy consumption and differences for test and reference cells.

4.3 Reducing the Off-Gas Suction Rate

To test the effects of changes in the energy loss through the off-gas system, the suction rate was reduced on one cell during some days in the winter season. The initial reduction mimicked summer conditions, with off-gas mass flow rates according to findings in Section 3.2. Towards the end of the test period, the suction was reduced even further, down to minimum viable rate while still maintaining a sealed superstructure on the cell.

Off-gas temperature and gas suction rates were monitored continuously during the test period. With the first reduction, the off-gas temperature response was only marginal, see Figure 12. However, with the last change, there was an evident increase in the temperature. The test cell voltage showed a similar response, see Figure 13, with minimal effect after the first off-gas reduction and a small, but clear change when reducing the rate even further. Other studies also support that alteration of the cell heat balance would require significant changes to the off-gas flow rate [14, 15].

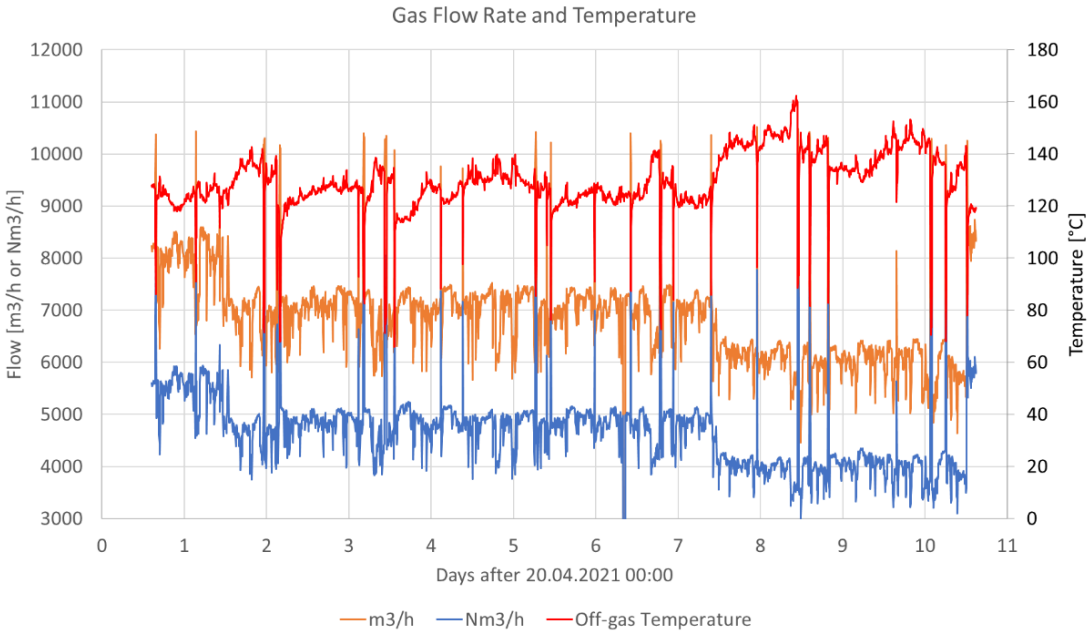

Figure 12. Energy consumption and differences for test and reference cells.

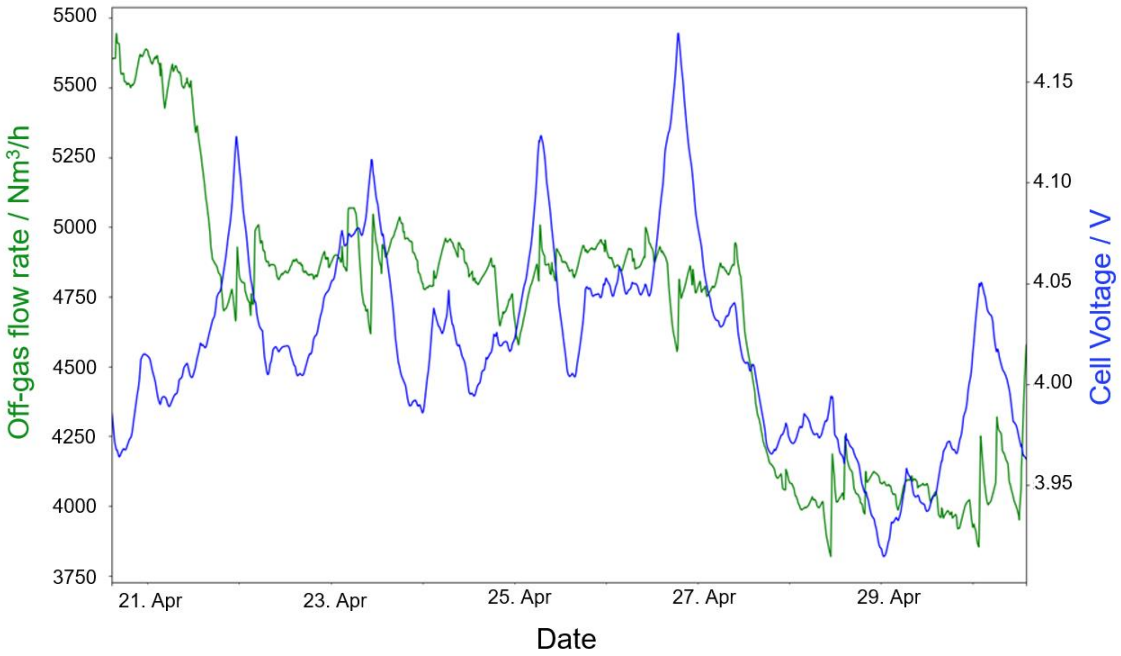

Figure 13. Off-gas flow rate (green) and cell voltage (blue) during the test period.

5. Discussion and Further Work

The recent years' work on understanding the influence of ambient conditions on aluminium cells is starting to show promising results. Observations and long-time measurements indicate that some cells' response to changes in ambient temperature is considerably more pronounced than what has been anticipated previously – commonly referred to as the "summer effect". Models that support these facts are also emerging.

This paper has presented three hypotheses around what could contribute to warmer cells during summer. Theoretical reviews showed that the convective part of the heat transfer coefficient decreases with higher temperatures. This is counteracted by the radiative term, and the net heat transfer coefficient is only marginally dependent on ambient temperature. The findings are also supported by CFD calculations, where the results confirm that pot shell temperatures increase approximately equal to the ambient temperature if the heat flux through the side is assumed constant. The actual local effects are dependent on the initial pot shell temperatures, as radiation becomes more important and starts to dominate in higher temperature regimes.

Experiments during the last two summers have shown that even small amounts of additional air between the cradles can impact the cells' performance. This suggests that increasing the external heat transfer coefficient could, to some extent, counteract the "summer effect".

Tests with reduced off-gas suction rates indicated that difference in mass flow rate from winter to summer only have a marginal effect on the cells' heat balance, also confirmed by other studies.

Even though the measurements and the analyses show that the impact of ambient temperature, ventilation rate and reduced off-gas amount cannot explain the observations, they still give contributions and push the cells towards a hotter state. Warmer pot shells mean that heat evacuation becomes harder, and the cells must compensate through e.g. thinner side ledge or reduced ACD. A third and relatively new hypothesis around CE as function of ACD suggests that even a small reduction can influence the cell energy balance, provided that the cell already is close to the lower ACD limit. This could lead to a regulation paradox where a reduction in ACD, normally

decreasing the heat generation in the cell, instead would increase the heat production. If correct, this indicates that we are approaching the limit of the interpolar distance. The project will be followed up with more tests and measurement. We would especially like to push the ACD during wintertime to see if this paradox can be realized.

6. Acknowledgement

The authors would particularly thank our colleagues Bjørn Petter Moxnes, Nils-Håvard Giskeødegård and Øyvind Hansen for their contributions and help to conduct the measurement campaigns, and Jørn L. Rutlin for providing data on earlier pot shell temperature measurements. Our thanks to the Research Council of Norway for providing financial support through grant 317855 Profitable and Sustainable Cell Technology for Hydro Aluminium smelters (RÉAL). Permission from Hydro Aluminium to publish this work is greatly appreciated.

7. References

1. Bjørn Moxnes, Halvor Kvande, and Asbjørn Solheim, Experience and challenges with amperage increase in Hydro Aluminium potlines, *Light Metals* 2007, 263-268.
2. Pierre Reny et al., Hydro's New Karmøy Technology Pilot: Start-Up and Early Operation, *Light Metals* 2021, 608-617.
3. Asgeir Bardal et al., HAL 4e - Hydro's new generation cell technology, *Light Metals* 2009, 371-375.
4. Elin Haugland, Håvard Børset, Håvard Gikling, and Helge Høie, Effects of ambient temperature and ventilation on shell temperature, heat balance and side ledge of an alumina reduction cell, *Light Metals* 2002, 269-276.
5. Torstein Haarberg, Asbjørn Solheim, Stein T. Johansen, and Per A. Solli, Effect of anodic gas release on current efficiency in Hall-Heroult cells, *Light Metals* 1998, 475-481.
6. Geoff Bearne, A. Jenkin, L. Knapp, and I. Saeed, The impact of cell geometry on cell performance, *Light Metals* 1995, 375-380.
7. Stuart W. Churchill, and Humbert H. S. Chu, Correlating equations for laminar and turbulent free convection from a vertical plate, *International Journal of Heat and Mass Transfer* 1975, 1323-1329.
8. J.R. Welty, C.E. Wicks, and R.E. Wilson, *Fundamentals of momentum, heat, and mass transfer*, John Wiley & Sons, Inc., Singapore, 1984.
9. EngineersEdge (retrieved June, 2022): https://www.engineersedge.com/heat_transfer/flat_plate_heat_transfer_convected_13956.htm
10. Sverre Rolseth, Tugrul Muftuoglu, Asbjørn Solheim, and Jomar Thonstad, Current efficiency at short anode-cathode distance in aluminium electrolysis, *Light Metals* 1986, 517-523.
11. Asbjørn Solheim, Current efficiency in aluminium reduction cells: Theories, models, concepts, and speculations, *Light Metals* 2014, 753-758.
12. Asbjørn Solheim, Arguments for keeping uniform alumina concentration and anode-cathode distance in aluminium electrolysis cells, *Proceedings of 40th International ICSOBA Conference*, Athens, Greece, 10 – 14 October, 2022 (this volume).
13. NIST-JANAF Thermochemical Tables, https://janaf.nist.gov/ (Retrieved May, 2022).
14. Alexander Arkhipov, Ievgen Necheporenko, Alexander Mukhanov, Nadia Ahli, and Khawla AlMarzooqi, Modelling study of exhaust rate impact on heat loss from aluminium reduction cells, *Light Metals* 2019, 625-635.
15. Sara T. Mathisen, Elin Haugland, Top heat losses at reduced duct flow. Measurement campaign July-August 2004. *Internal Report 05Q_AA0,* 2005.